ACS APPLIED MATERIALS & INTERFACES

Research Article

www.acsami.org

Design and Fabrication of Branched Polyamine Functionalized Mesoporous Silica: An Efficient Absorbent for Water Remediation

Sana Nayab,[§] Aleeza Farrukh,[∥,‡] Zehra Oluz,[⊥] Eylül Tuncel,[⊥] Saadia Rashid Tariq,[§] Habib ur Rahman,[‡] Katrin Kirchhoff,[∥] Hatice Duran,[⊥] and Basit Yameen*[,‡,†]

[§]Department of Chemistry, Lahore College for Women University, Jail Road, Lahore, Punjab 54000, Pakistan

[‡]Department of Chemistry, SBA School of Science and Engineering, Lahore University of Management Sciences, Lahore, Punjab 54792, Pakistan

[⊥]Department of Materials Science & Nanotechnology Engineering, TOBB University of Economics and Technology, Sogutozu Cad. 43, Ankara, 06560, Turkey

[∥]Max-Planck-Institut für Polymerforschung, Ackermannweg 10, Mainz, Rhineland-Palatinate 55128, Germany

ABSTRACT: A novel branched polyamine (polyethyleneimine, PEI) functionalized mesoporous silica (MS) adsorbent is developed via a facile "grafting-to" approach. X-ray photoelectron spectroscopy (XPS) and Fourier transform infrared (FT-IR) spectroscopy verified the effective surface functionalization of MS with monolayer and polymer. The transmission electron microscopy (TEM) was employed to reveal the morphology of the fabricated materials. The adsorption behavior of the polyamine functionalized mesoporous silica (MS-PEI) is assessed against anionic dyes. The adsorbent characteristics of MS-PEI are compared with a monolayer platform comprising of 3-aminopropyltriethoxy silane (APTES) functionalized mesoporous silica (MS-APTES). The adsorption behavior of the MS-PEI and MS-APTES toward anionic dyes is further evaluated by studying the effect of adsorbent dosage, pH, contact time, and temperature. Langmuir and Freundlich isotherm models are employed to understand the adsorption mechanism. The obtained kinetic data support a pseudo-second-order adsorption behavior for both monolayer and polymer functionalized MS. The associated thermodynamic parameters ($\Delta G°$, $\Delta H°$, and $\Delta S°$) reveal that the process of adsorption with MS-PEI is more spontaneous and energetically favored as compared to the adsorption with MS-APTES. Taken together, the novel adsorbent system derived from a combination of MS and branched polymer (MS-PEI) shows the higher absorption efficiency and capacity toward the anionic dyes than the monolayer based adsorbent (MS-APTES).

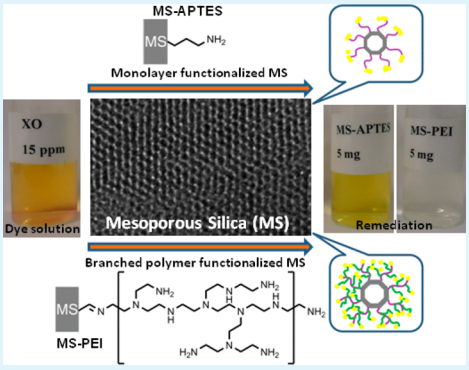

KEYWORDS: *mesoporous silica, branched polyamine, surface modification, adsorbent, water remediation*

INTRODUCTION

Mesoporous silica based materials are being investigated for a variety of different applications such as catalysis,[1] drug delivery,[2] adsorption,[3] and separation.[4] These materials are typically synthesized with tunable pore size and geometry in the presence of different cationic/anionic surfactants, which act as templates.[5,6] A large variety of mesoporous silica including hexagonal, cubic, dodecagonal, or platelet geometries has been investigated for various applications.[5] The hexagonal MCM-41 mesoporous silica has been prepared by using cationic surfactants as cetyltrimethylammonium bromide (CTAB).[7] Mesoporous materials have emerged as promising adsorbents for the water remediation and offer advantages such as high surface area, surface reactivity, structural stability, and regular channel-type structures.[8−10] It is well-known that silica based materials have a negative charge surface due to the presence of Si−OH groups, which prevents the adsorption of negatively charged adsorbates.[11,12] Therefore, the effectiveness of mesoporous silica in the adsorption processes is highly dependent on the surface functionalization of the silica network with functional groups that are suitable for adsorption of specific substances. A variety of surface functionalized mesoporous silica has been explored for adsorption of heavy metal ions and cationic and anionic organic materials.[3,13−19]

Among the organic pollutant, dye contaminants have caused serious pollution to water resources and the removal of dyes from wastewater has become a major focus of research. Even the presence of a small concentration of dyes (less than 1 mg L^{-1}) is highly visible and considered to be intolerable.[20] Many of these dyes are carcinogenic and toxic. In addition, such dyes are resistant to degradation by light, chemical, biological, and other exposures.[21,22] There are various techniques that are used for the remediation of dye wastewater such as oxidation, ozonation,[23] coagulation and flocculation,[24] membrane separa-

Received: January 7, 2014
Accepted: February 24, 2014
Published: February 24, 2014

Scheme 1. Schematic Illustration of the Synthesis of APTES Based Monolayer (MS-APTES) and PEI Based Branched Polymer (MS-PEI) Functionalized Mesoporous Silica

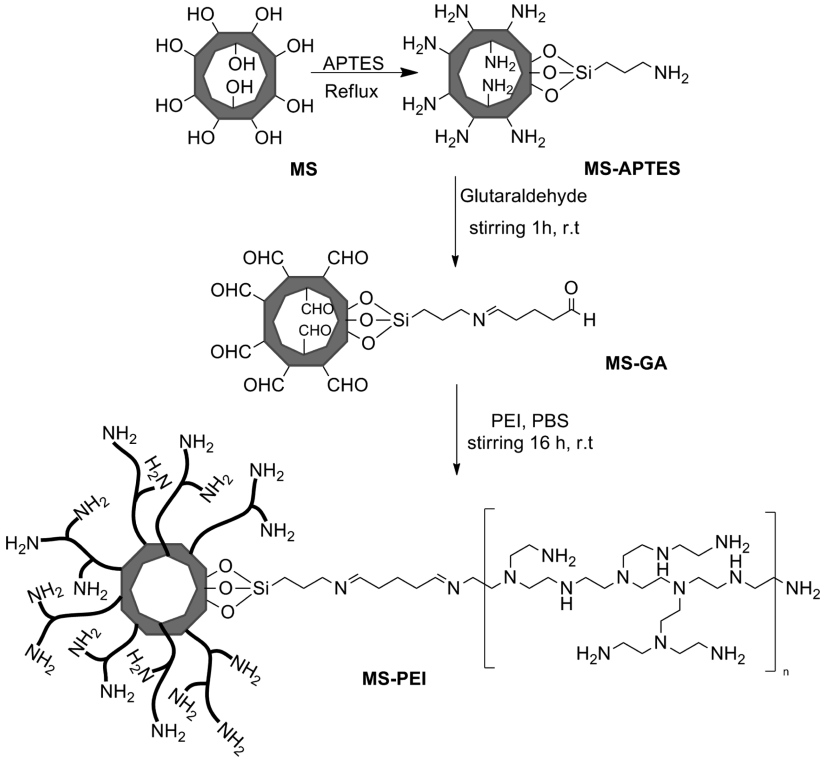

tion,[25] and adsorption.[26] Among these techniques, adsorption is considered to be the most frequent and proficient method for dye removal from wastewater.

The amine functionalization of mesoporous silica has been particularly explored for the water remediation purposes because of the chelating nature of the amino groups. Various physical and covalent strategies have been developed to achieve amine functionalized mesoporous silica.[27−30] Recently, "grafting-from" approach based on surface initiated ring-opening polymerization has been considered as an alternate route to polyamine functionalized mesoporous silica.[31] It is, however, well established that the widely employed "grafting-to" approach of surface tethering of polymers is simple and practical and can be conducted under mild conditions.[32] Exploiting this opportunity, we herein report an unprecedented branched polymer (polyethyleneimine, PEI) based polyamine functionalized MCM-41 mesoporous silica (MS-PEI) as a potential absorbent for remediation of anionic contaminants. Adsorption behavior of MS-PEI was evaluated against two anionic dyes, i.e., Alizarin Red S and Xylenol Orange. The adsorption behavior of MS-PEI was also compared with and found superior to the 3-aminopropyltriethyoxysilane (APTES) derived monolayer based amine functionalized MS (MS-APTES). The improved adsorption characteristics of MS-PEI adsorbent were attributed to relatively higher surface functional group density, inherent with the polymeric nature of surface functionalization, leading to a larger number of active adsorption sites on the surface of MS-PEI. The effects of various parameters such as chemical modification, adsorbent dosage, contact time, pH, temperature, and concentration of dye solution were also studied in detail. The mechanistic nature of the adsorption process was estimated by applying the Langmuir and Freundlich isotherm models. In addition, the thermodynamics and kinetic parameters associated with the adsorption process were also evaluated.

EXPERIMENTAL SECTION

Materials and Methods. 1-Hexadecyl trimethylammonium bromide (CTAB), aqueous ammonia (NH_3, 35%), tetraethyl orthosilicate (TEOS, 99%), toluene (99%), 3-aminopropyltriethoxysilane (APTES, 98%), glutaraldehyde (GA, 50% in water), branched polyethyleneimine (PEI, $M_w \sim 25$ KDa by LS, $M_n \sim 10$ KDa by GPC, data from Sigma Aldrich), sodium dihydrogen phosphate (NaH_2PO_4, 97%), sodium hydrogen phosphate (Na_2HPO_4, 98%), ethanol (>99%), and methanol were purchased from Sigma Aldrich, Germany. Acetic acid was obtained from Merck, Germany. Alizarin red S (ARS) was purchased from Eyer chemical reagents, China. Xylenol Orange (XO) was received from Unichem chemical reagents. Toluene was dried using Na/benzophenone prior to use.

Synthesis of Mesoporous Silica (MS). The MS was prepared according to the method previously reported.[33] CTAB (4g) was dissolved in 1.1 M NH_4OH (1000 mL), and TEOS (16 mL, 71.65 mmol) was added to this solution under vigorous stirring. Precipitates were formed within 10 min of adding the TEOS (silica precursor), and the mixture was allowed to age for 24 h at room temperature. The precipitates were then collected by filtration and thoroughly washed with water by centrifugation at 4000 rpm for 20 min. The particles were dried overnight at 323 K before calcination at 823 K to remove the organic template.

Synthesis of Monoamine Modified Silica (MS-APTES). APTES coated mesoporous silica (MS-APTES) was prepared according to the reported procedure.[34] Calcined MS (2.5g) was refluxed in dry toluene (250 mL) containing 0.1 mol of APTES for 16 h. The product was filtered, washed with toluene by centrifugation for 20 min at 4000 rpm, and oven-dried at 383 K for 18 h.

Surface Modification of Silica with Glutaraldehyde (MS-GA). Surface modification of MS-APTES with glutaraldehyde was accomplished according to the previously reported method.[35] Briefly, MS-APTES (5g) was suspended in 5% glutaraldehyde aqueous

solution (100 mL) at room temperature for 1 h. The aldehyde functionalized MS was washed with an excess of deionized water and acetone sequentially by centrifugation for 20 min at 4000 rpm to remove residual glutaraldehyde and dried in an oven at 373 K for 2 h.

Functionalization of Silica with Branched Polyethyleneimide (MS-PEI). MS-GA (3g) was stirred in phosphate buffer solution (500 mL, pH = 7) containing PEI (1.0 mg/mL) for 16 h at room temperature. Branched PEI tethered silica particles were washed several times with deionized water by centrifugation for 20 min at 4000 rpm to remove physically adsorbed PEI and dried overnight in an oven at 313 K.

Characterization. Attenuated total reflection ATR-FTIR spectra were recorded on Alpha Bruker Germany, spectrometer. Transmission electron microscopic (TEM) images were obtained by using FEI Tecnai G2 F20 instrument with an accelerating voltage of 200 kV. Samples were prepared by drop casting two to three drops of particle dispersions in ethanol onto a carbon coated copper TEM grid. X-ray photoelectron spectroscopy (XPS) measurements were carried out using Thermo Scientific K-Alpha. The Mg Kα (1253.6 eV) X-ray source was operated at 300 W. Pass energy of 117.40 eV was used for the survey scans. The spectra were recorded using a 60° take off angle relative to the surface normal. The UV/vis absorption spectra of the dyes were recorded using a Shimadzu UV-1800 spectrophotometer.

Adsorption Studies. The dye adsorption capacities of MS-APTES and MS-PEI were studied by using various amounts of adsorbents. Functionalized mesoporous silica particles (5−20 mg) were shaken at room temperature (400 rpm) with 10 mL aqueous dye solutions of known initial concentration (15 ppm) at optimized contact time and pH (pH = 6, t = 15 min for ARS while pH = 4, t = 2 min for XO). At the end of the adsorption period, the supernatant solutions were filtered and the concentration of each dye in the supernatant solutions before and after the adsorption was determined using a calibration curve obtained by employing a UV/vis spectrophotometer at λ_{max} of 470 nm for ARS and 436 nm for XO.

The amount of dye adsorbed at equilibrium q_e (mg/g) was calculated from the following equation.

$$q_e = \frac{(C_o - C_e)V}{W} \quad (1)$$

where q_e is the adsorption capacity (mg/g) of the adsorbent at equilibrium, C_o and C_e (mg/g) are the initial and equilibrium concentrations of solute, V is the volume of the aqueous solution in liters, and W is the mass in grams of the adsorbent used.[36]

RESULT AND DISCUSSION

A surfactant based template assisted method was used for the fabrication of MS. The surface functionalization of MS with APTES followed by the reaction with glutaraldehyde led to the MS with surface aldehyde groups. The surface aldehyde groups were subsequently used for covalently tethering the branched PEI at the surface of MS via imine linkage. The overall surface functionalization strategy is illustrated in Scheme 1.

The surface functionalization was supported by the ATR-FTIR spectroscopic analyses. The characteristic bands for Si−O−Si stretching vibration were clearly observed at 1047 and 791 cm^{-1} (Figure 1). The surface modification of MS with APTES was confirmed by the presence of $-CH_2$ deformation at 1465 cm^{-1} and $-NH_3^+$ band at 1563 cm^{-1} and most importantly by the existence of NH_2 bending at 1640 cm^{-1} and C−H (CH_2) stretching at 2930 cm^{-1}. Similarly, MS with PEI resulted in the appearance of absorption band at 1647 cm^{-1}, which can be attributed to the stretching vibration of C═N while stretching vibration of N−H was observed at 3340 cm^{-1}.

The surface chemical modifications were further substantiated by employing XPS analysis (Figure 2). The survey scan of MS-APTES showed signals at 153 and 101 eV, which correspond to the binding energies of Si2s and Si2p orbitals

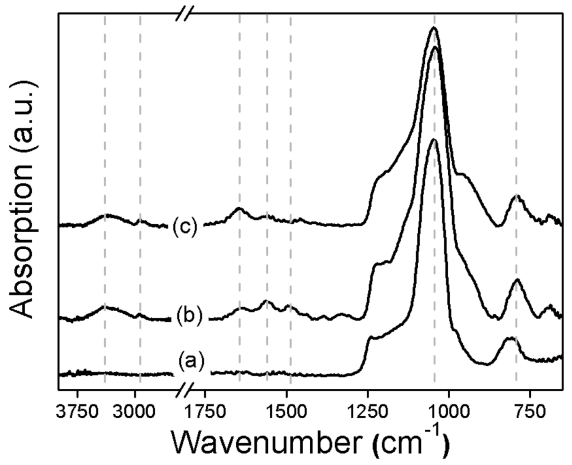

Figure 1. ATR-FTIR spectra of as synthesized MS (a) and MS functionalized with glutaraldehyde (b) and PEI (c).

of Si. The signal for the C1s and O1s orbitals of the carbon and oxygen contents of MS-APTES can be observed at 284 and 533 eV (Figure 2a).[37] The presence of N1s orbital signal at 400 eV in the XPS survey scan of MS-APTES validates the amine functionalization of MS. The subsequent immobilization of glutaraldehyde and PEI was ascertained by a change in the N/C ratio. The N/C ratio for MS-PEI (N/C: 0.16) was 2.5 times higher than the N/C observed for the glutaraldehyde functionalized MS (N/C: 0.064). The higher nitrogen content in the case of MS-PEI was in agreement with the effective surface immobilization of PEI.

The TEM imaging revealed the mesoporous morphology of the employed MS (Figure 3). The size of the particles constituting the MS ranged between 200 and 1000 nm. The mesoporous nature of the MS was also retained during functionalization with the APTES (Figure 3c). Grafting of PEI on the surface of MS led to the appearance of a thin polymer film uniformly covering the whole surface of mesoporous silica (Figure 3d). Taken together, Fourier transform infrared (FT-IR), XPS, and TEM analyses corroborate the surface chemical functionalization of MS.

After successful fabrication and characterization of the branched PEI functionalized MS, its adsorption behavior was investigated. APTES functionalized MS, with monolayer based amine surface functional groups, was employed as a reference material.

Effect of Adsorbent Dosage. The effect of adsorbent dosage on the adsorption of dyes was studied at room temperature for different amounts of particles (5, 10, 15, and 20 mg). In order to compare the efficiency of the prepared adsorbents, the specified amounts of MS-APTES and MS-PEI were separately added to 10 mL of 15 ppm dye solutions at room temperature with optimized contact time and pH (15 min, pH = 6 for ARS, and 2 min, pH = 4 for XO). The dye removal percentage increased with the increase in amount of adsorbent.[38] For both dyes used, MS-PEI showed higher adsorption capacity as compared to the MS-APTES (Figure 4). Both the adsorbents (MS-PEI and MS-APTES) reached to their maximum adsorption capacity at 15 mg for ARS dye (99% and 89%, respectively) and 20 mg for XO dye (89% and 77%, respectively).

The electrostatic charge on the ARS molecules is more stable than on the XO molecules (SO_3^- vs COO^-) (Figure 5),

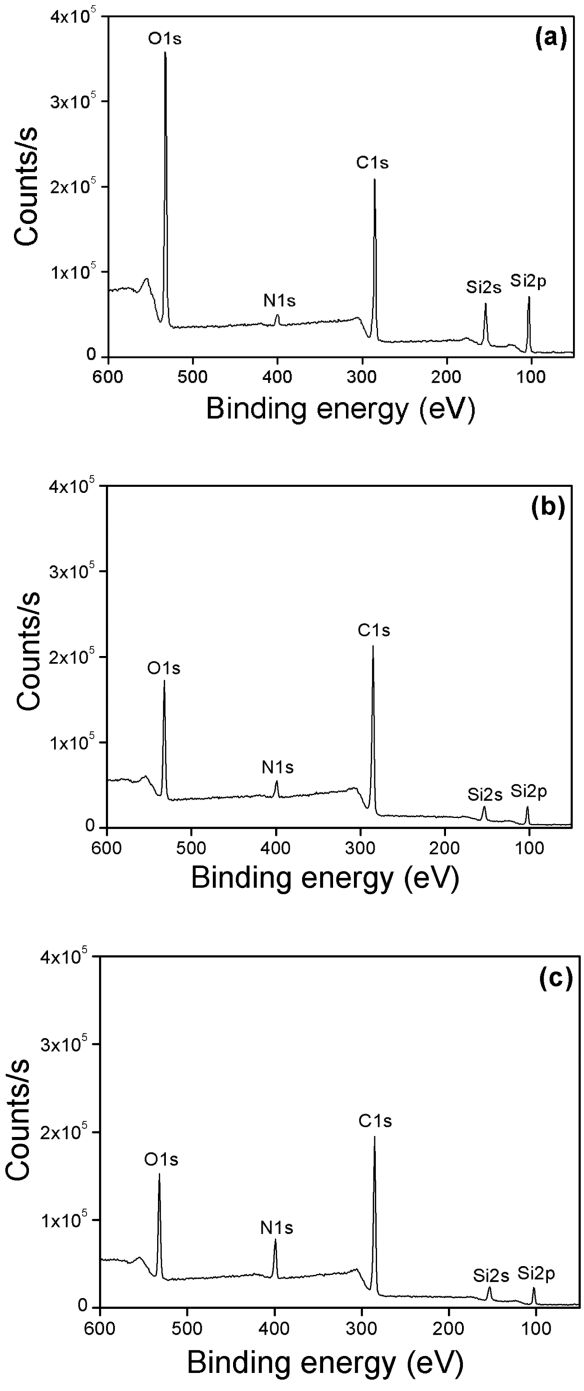

Figure 2. XPS survey scans of APTES (a), glutaraldehyde (b), and PEI (c) functionalized MS.

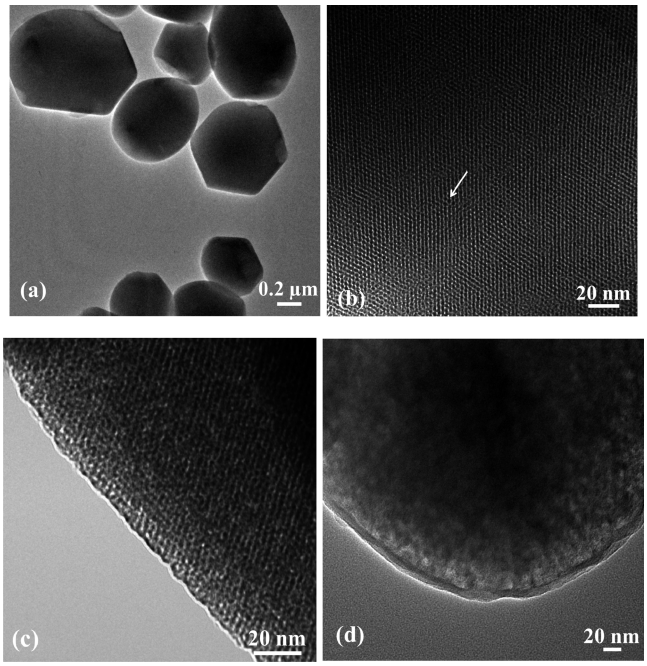

Figure 3. TEM image of as synthesized MS (a); HR-TEM images of as synthesized MS (b) and MS functionalized with APTES (c) and PEI (d).

therefore; both the adsorbents exhibited higher removal capacity toward ARS.

Effect of Contact Time. For an ideal adsorbent for water treatment, it needs to show rapid uptake of pollutants and reach the equilibrium in short time.[39] To investigate the effect of contact time on the adsorption of dyes, the functionalized adsorbents (10 mg for ARS and 5 mg for XO) were added to 10 mL of 15 ppm dye solution for time periods ranging from 5 to 30 min for ARS (at pH = 6) and 1 to 5 min for XO (at pH = 4). It was noticed that, for both dyes, uptake increases with the increase in contact time. However, at any given time point, the MS-PEI exhibited higher removal capacity than APTES. MS-PEI exhibited almost complete adsorption of ARS from 15 ppm solution after 30 min, whereas adsorption was 90% in the case of MS-APTES under similar conditions. Adsorption of XO was up to 88% for MS-PEI and 68% for MS-APTES after 5 min (Figure 6). This was the maximum adsorption that could be achieved for both adsorbents in the case of XO, and further increase in contact time did not increase the adsorption indicating the advent of adsorption equilibrium. MS-PEI showed higher adsorption capacity with respect to MS-APTES due to the higher surface functional group density at adsorption sites.

Effect of Temperature. Temperature has a significant effect on the adsorption process. To study the effect of temperature on the uptake of dyes, adsorption experiments were carried out at different temperatures (ranging from 25 to 65 °C). Both adsorbents (10 mg, pH = 6, t = 15 min for ARS, and 5 mg, pH = 4, t = 2 min for XO) were added to the 10 mL of 15 ppm dye solutions. For both the adsorbents (MS-PEI and MS-APTES), an increase in temperature only slightly decreased the adsorption capacity and maximum adsorption was achieved at room temperature (98% and 88% for ARS and 83% and 65% for XO, respectively; Figure 7). This behavior revealed an exothermic nature of the adsorption process. The weakening of physical interactions between dyes and active adsorbent sites could be the significant contributor toward a decrease in adsorption capacity with an increase in the temperature. The aqueous solubility of solutes generally increases with the increase in temperature, therefore impeding the adsorption process.[40]

Effect of pH. The pH of the solution is a key parameter in regulating the adsorption of charged moieties, by altering the surface charge of the adsorbent and the degree of ionization of the dyes. The effect of pH on the adsorption of anionic dyes ARS and XO was studied systematically. For this purpose, solutions were prepared in the pH range of 2−12. The pH of solutions was adjusted by using 0.1 M HCl and 0.1 M NaOH.

dx.doi.org/10.1021/am500123k | ACS Appl. Mater. Interfaces 2014, 6, 4408−4417

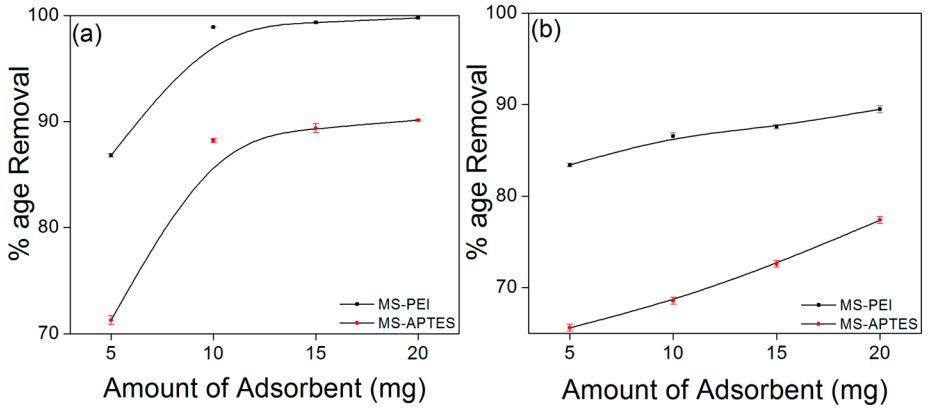

Figure 4. Effect of adsorbent dosage on % age of dye removal: ARS (pH = 6, t = 15 min, T = 25 °C) (a); XO (pH = 4, t = 2 min, T = 25 °C) by MS-APTES and MS-PEI (b). The solid curve is a guide to the eye.

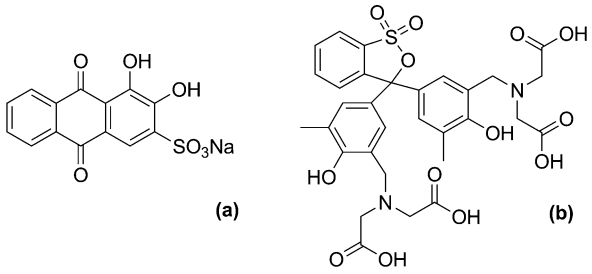

Figure 5. Structure of dyes: Alizarin Red S (a); Xylenol Orange (b).

The adsorption capacity of MS-PEI and MS-APTES toward ARS (15 ppm, 10 mL, t = 15 min, 10 mg adsorbent) initially increased as the pH of the solution was increased from 2 and reached a maximum at 6. At pH 6, the surface positive charge on the adsorbents, due to the protonation of the amino groups, and the negative charge on the ARS seem to be in the right combination to give maximum adsorption (98% for MS-PEI and 88% for MS-APTES).[41] A further increase in the pH resulted in the decrease of adsorption capacity, presumably because of the deprotonation of the surface amino groups and protonation of the acidic functional groups of ARS, leading to an electrostatic repulsion between adsorbent and the adsorbate. A similar trend was observed for the XO (15 ppm, 10 mL, t = 2 min, 5 mg adsorbent) where both adsorbents (MS-PEI and MS-PEI) showed maximum adsorption capacity (83% and 65% respectively) at pH 4 (Figure 8).

Adsorption Isotherms. In the adsorption process, the distribution of solute between the solid and liquid phase and measure of the distribution coefficient can be studied by employing different adsorption isotherms. Langmuir and Freundlich isotherm models are so far most frequently used for interpretation of adsorption process. The Langmuir theory depicts that adsorption occurs at specific homogeneous sites within the adsorbent, and once a dye molecule resides at a site, no further adsorption takes place at that site. In addition, this model assumes the monolayer nature of the adsorption on homogeneous adsorbent, where all the sorption sites are identical. The linear form of the Langmuir equation is:

$$\frac{C_e}{q_e} = \frac{1}{q_{max} b} + \frac{C_e}{q_{max}} \quad (2)$$

where q_e is the amount of adsorbate adsorbed per unit mass of adsorbent (mg/g), C_e is the equilibrium concentration of the adsorbate (mg L^{-1}), and q_{max} (mg g^{-1}) and b (L mg^{-1}) are the Langmuir constants related to maximum monolayer adsorption capacity and energy change in adsorption, respectively.[36,39]

The feasibility of the adsorption can be expressed in terms of a dimensionless factor called separation factor (R_L), which is defined by the following equation:

$$R_L = \frac{1}{bC_o + 1} \quad (3)$$

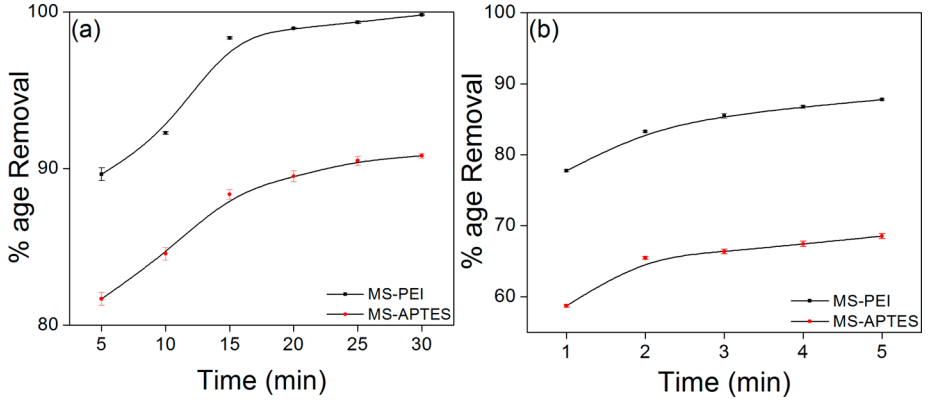

Figure 6. Effect of time on % age of dye removal: ARS (pH = 6, T = 25 °C, amount of adsorbent = 10 mg) (a); XO (pH = 4, T = 25 °C, amount of adsorbent = 5 mg) by MS-APTES and MS-PEI (b). The solid curve is a guide to the eye.

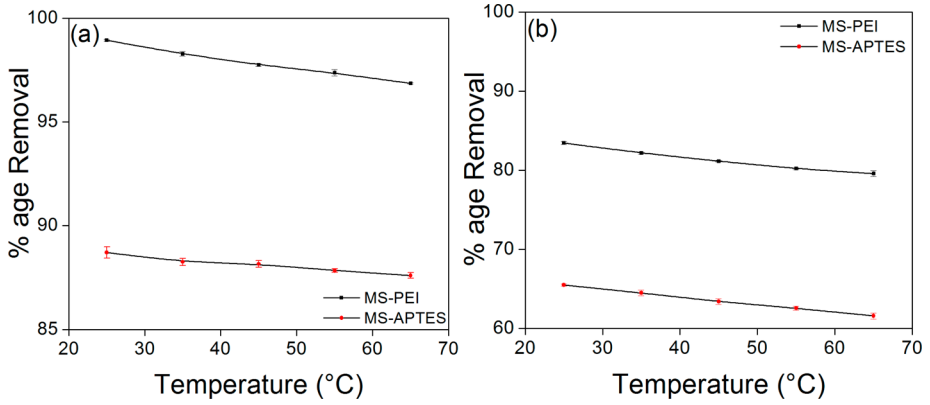

Figure 7. Effect of temperature on % age of dye removal: ARS (pH = 6, t = 15 min, amount of adsorbent = 10 mg) (a); XO (pH = 4, t = 2 min, amount of adsorbent = 5 mg) by MS-APTES and MS-PEI (b). The solid curve is a guide to the eye.

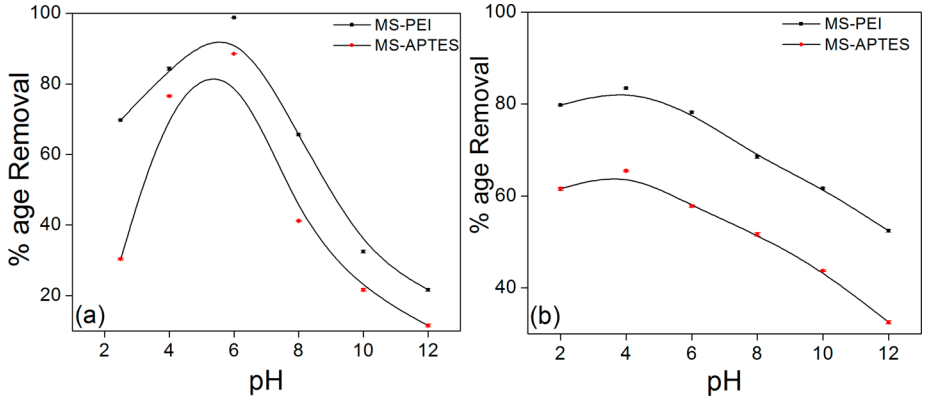

Figure 8. Effect of pH on % age of dye removal: ARS (t = 15 min, T = 25 °C, amount of adsorbent = 10 mg) (a); XO (t = 2 min, T = 25 °C, amount of adsorbent = 5 mg) by MS-APTES and MS-PEI (b). The solid curve is a guide to the eye.

Table 1. Langmuir and Freundlich Isotherms Parameters for the Adsorption of ARS and XO on MS-APTES and MS-PEI

MS-APTES				MS-PEI			
	parameters	Alizarin Red S	Xylenol Orange		parameters	Alizarin Red S	Xylenol Orange
Langmuir	q_{max} (mg g^{-1})	35.71 ± 2.40	65.23 ± 1.72	Langmuir	q_{max} (mg g^{-1})	147.28 ± 7.36	186.92 ± 2.78
	b (L mg^{-1})	0.44 ± 0.11	0.11 ± 0.06		b (L mg^{-1})	0.10 ± 0.05	0.06 ± 0.02
	R_L	0.34 ± 0.02	0.65 ± 0.11		R_L	0.66 ± 0.14	0.70 ± 0.08
	R^2	0.845	0.868		R^2	0.987	0.973
Freundlich	K_f (mg g^{-1})	11.98 ± 1.21	7.03 ± 1.5	Freundlich	K_f (mg g^{-1})	13.41 ± 1.08	11.76 ± 1.25
	$1/n$	0.36 ± 0.08	0.70 ± 0.20		$1/n$	0.93 ± 0.03	0.88 ± 0.15
	R^2	0.738	0.805		R^2	0.976	0.978

where C_o (mg L^{-1}) is the initial adsorbate concentration. The value of R_L indicates the shape of the isotherm to be either unfavorable ($R_L > 1$), linear ($R_L = 1$), favorable ($0 < R_L < 1$), or irreversible ($R_L = 0$).[39]

The Freundlich isotherm model is an empirical equation which describes that the adsorption process occurs at heterogeneous surfaces and is not limited to the formation of the monolayer. This isotherm also explains that the sorption sites with greater affinity are occupied first. The linear form of this model is written as:

$$\log q_e = \log K_f + \frac{1}{n}\log C_e \quad (4)$$

where q_e represents equilibrium dye concentration on an adsorbent (mg g^{-1}), K_f is the Freundlich constant, which corresponds to adsorption capacity (mg g^{-1}), and $1/n$ is the heterogeneity factor. The slope, $1/n$, with favorable range between 0 and 1, is a measure of adsorption intensity and surface heterogeneity. C_e represents equilibrium dye concentration in solutions (mg L^{-1}).[36]

The relationship between adsorbent and adsorbate was established by applying the Langmuir and the Freundlich models. The maximum adsorption capacities of MS-PEI for ARS and XO dye molecules were calculated as 147.275 and 186.920 mg g^{-1}, respectively (Table 1). On the other hand, the maximum adsorption of MS-APTES was 3−4 times less than MS-PEI. This showed that the adsorption capacity of MS-PEI is much higher than MS-APTES. The calculated R_L was in the range of $0 < R_L < 1$ for both the functional MS, indicating a favorable adsorption of both dye molecules (ARS and XO). In comparison to a previous report[42] that employed a PEI functionalized nonmesoporous silica nanoparticle for remediation against anionic dye, the present study shows a clear advantage of higher adsorption capacity for the PEI function-

dx.doi.org/10.1021/am500123k | ACS Appl. Mater. Interfaces 2014, 6, 4408−4417

Table 2. Parameters of Pseudo-First-Order and Pseudo-Second-Order Kinetics for the Adsorption of ARS and XO on MS-APTES and MS-PEI

MS-APTES				MS-PEI			
	parameters	Alizarin Red S	Xylenol Orange		parameters	Alizarin Red S	Xylenol Orange
pseudo-first-order	q_e (mg g^{-1}) calculated	1.86 ± 0.18	7.78 ± 0.13	pseudo-first-order	q_e (mg g^{-1}) calculated	2.15 ± 0.16	6.32 ± 0.26
	k_1 (min^{-1})	0.13 ± 0.02	0.69 ± 0.11		k_1 (min^{-1})	0.15 ± 0.02	0.76 ± 0.21
	R^2	0.869	0.925		R^2	0.929	0.998
pseudo-second-order	q_e (mg g^{-1}) calculated	13.82 ± 0.70	21.34 ± 0.15	pseudo-second-order	q_e (mg g^{-1}) calculated	15.24 ± 0.4	27.20 ± 0.78
	k_2 (g/mg min)	0.15 ± 0.05	0.23 ± 0.03		k_2 (g/mg min)	0.13 ± 0.05	0.21 ± 0.03
	R^2	0.999	0.999		R^2	1	1

Table 3. Thermodynamic Parameters for the Adsorption of ARS and XO on MS-APTES and MS-PEI

MS-APTES			MS-PEI		
parameters	Alizarin Red S	Xylenol Orange	parameters	Alizarin Red S	Xylenol Orange
$\Delta G°$ (kJ mol^{-1})	−11.84 ± 1.02	−7.54 ± 0.93	$\Delta G°$ (kJ mol^{-1})	−24.37 ± 1.27	−13.08 ± 0.98
$\Delta H°$ (kJ mol^{-1})	−9.32 ± 0.13	−5.72 ± 0.27	$\Delta H°$ (kJ mol^{-1})	−19.41 ± 0.23	−10.75 ± 0.52
$\Delta S°$ (kJ $mol^{-1}K^{-1}$)	0.008 ± 0.003	0.006 ± 0.001	$\Delta S°$ (kJ $mol^{-1}K^{-1}$)	0.017 ± 0.004	0.008 ± 0.002
K	$1.13 \times 10^2 \pm 2.63$	$0.21 \times 10^2 \pm 0.69$	K	$1.95 \times 10^4 \pm 15.97$	$2.01 \times 10^2 \pm 1.76$

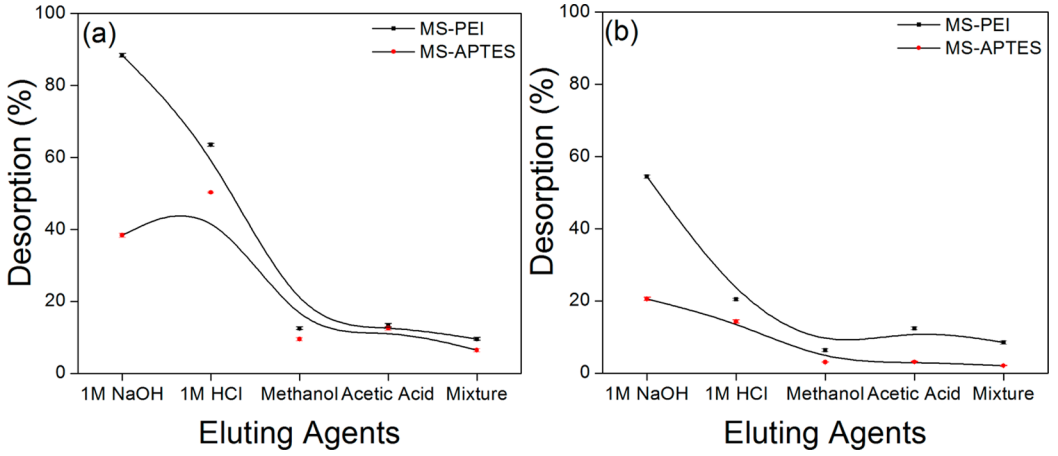

Figure 9. Effect of different eluting agents on desorption of dyes: ARS (T = 25 °C, t = 15 min) (a); XO (T = 25 °C, t = 2 min) from MS-APTES and MS-PEI (b).

alized mesoporous silica. In light of the reported literature[42−46] and to the best of our knowledge, this report is a first attempt that comprehensively reveals the superior adsorption capabilities of the PEI functionalized MPS as compared to the monolayer based amine functionalized MPS.

A comparison of the two isotherms based on the linear regression coefficient (R^2) values (Table 1) showed that the anionic dye adsorption on MS-APTES is better estimated by the Langmuir isotherm, whereas the dye adsorption on MS-PEI confirms nearly similar results (R^2) for both Langmuir and Freundlich isotherm models, under the concentration range studied.

Adsorption Kinetics. Adsorption kinetics assists in evaluating the rate and mechanism of mass transfer of adsorbate from liquid phase to solid adsorbent surface. Numerous kinetics models can be employed to explain the mechanism of solute sorption onto a sorbent. In the present study, pseudo-first-order and pseudo-second-order kinetics models were investigated (Table 2). The pseudo-first-order kinetics model has been extensively used to predict dye adsorption kinetics.[38] A linear form of the pseudo-first-order model was described by Lagergren:

$$\log(q_e - q_t) = \log q_e - \left(\frac{k_1}{2.303}\right)t \quad (5)$$

where q_e and q_t are the adsorption capacities (mg g^{-1}) at equilibrium and at time t, respectively, and k_1 is the rate constant of pseudo-first-order adsorption (min^{-1}).

The pseudo-second-order rate equation of McKay and Ho can be represented as:

$$\frac{t}{q_t} = \frac{1}{k_2 q_e^{\,2}} + \frac{1}{q_e}t \quad (6)$$

where the equilibrium adsorption capacity q_e and the pseudo-second-order constants k_2 (g/mg min) can be determined experimentally. From both comparison of experimental and theoretical calculation on an adsorbent and linear regression coefficient values, it can be seen that adsorption of anionic dyes may be best described by the pseudo-second-order kinetics model which assumes that the rate limiting step involves chemisorption of the adsorbate onto the adsorbent.

dx.doi.org/10.1021/am500123k | ACS Appl. Mater. Interfaces 2014, 6, 4408−4417

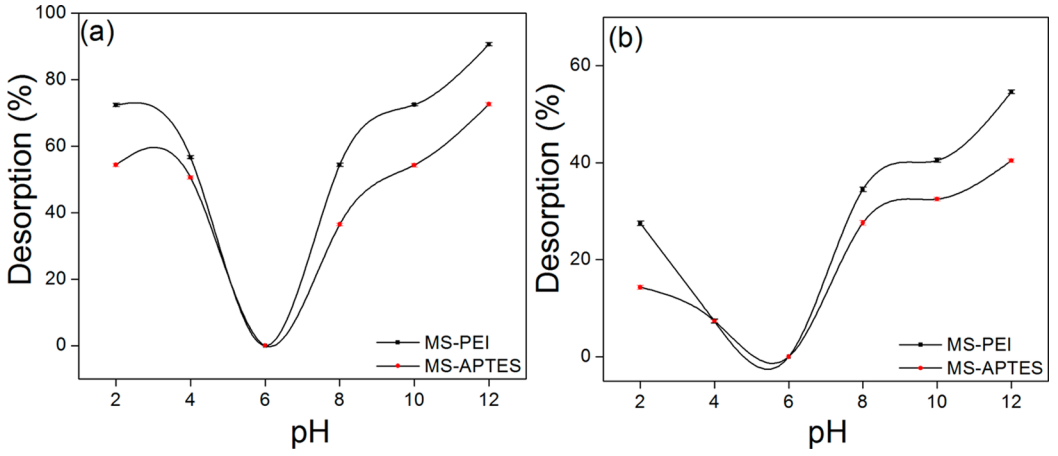

Figure 10. Effect of different pHs on desorption of dyes in water: ARS (T = 25 °C, t = 15 min, amount of adsorbent = 10 mg) (a); XO (T = 25 °C, t = 2 min, amount of adsorbent = 5 mg) from MS-APTES and MS-PEI (b).

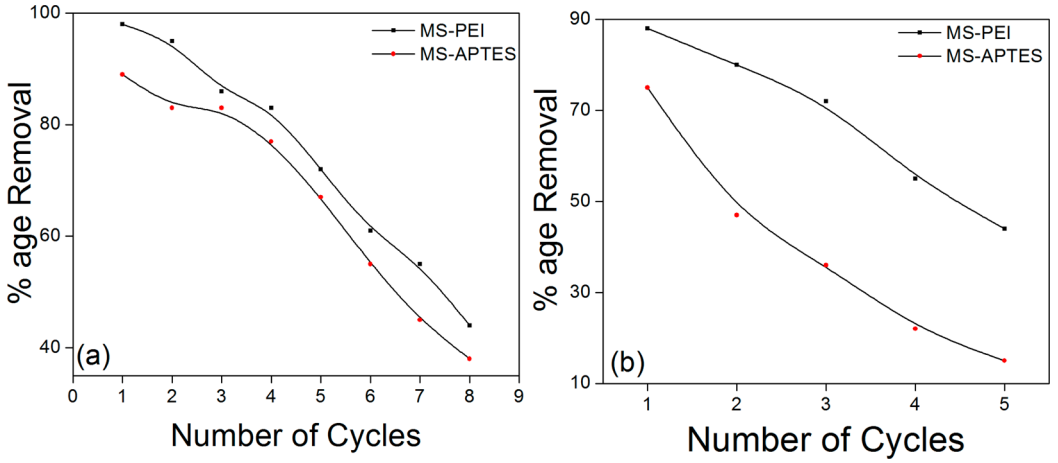

Figure 11. Reusability of MS-PEI and MS-APTES for adsorption studies: ARS (pH = 6, T = 25 °C, t = 15 min, amount of adsorbent = 10 mg) (a); XO (pH = 4, T = 25 °C, t = 2 min, amount of adsorbent = 5 mg) (b).

Adsorption Thermodynamics. In order to study the effect of temperature on the adsorption process, the values of the thermodynamic parameters such as the Gibbs' free energy ($\Delta G°$), the standard enthalpy change ($\Delta H°$), and the standard entropy change ($\Delta S°$) were investigated (Table 3). The magnitude of $\Delta G°$ was obtained from the following equation:

$$\Delta G° = -RT\ln K \tag{7}$$

where K is the equilibrium constant, T is the absolute temperature (K), and R is the universal gas constant (8.314 J/mol K).[41]

The enthalpy change $\Delta H°$ and $\Delta S°$ can be obtained from the van't Hoff equation:

$$\ln K = \frac{\Delta S°}{R} - \frac{\Delta H°}{RT} \tag{8}$$

The negative values of $\Delta G°$ confirmed that adsorption of dyes on both adsorbents was spontaneous. The negative values of $\Delta H°$ indicate the exothermic nature of adsorption processes. The positive values of $\Delta S°$ shows the increasing randomness at the surface of adsorbent during adsorption processes, which eventually leads to an increase in the adsorption efficiency. The rate constant (K) for MS-PEI is 2 orders of magnitude higher than the MS-APTES for ARS dye, and it is 1 order of magnitude higher for XO dye. Much larger values of K mean anionic dye adsorption on polyamine functionalized mesoporous nanoparticles is stronger and almost complete.

Desorption Studies. Sorbent regeneration is important in the estimation of the competitiveness of the adsorbent system. The desorption studies were carried out by employing different organic solvents and also in acidic, neutral, and alkaline media. The desorption of dyes was carried out by separately washing the ARS (T = 25 °C, t = 15 min) and XO (T = 25 °C, t = 2 min) loaded adsorbents with 10 mL each of 1 M HCl, 1 M NaOH, methanol, acetic acid, and a mixture of methanol (0.5 mL) with concentrated acetic acid (9.5 mL) (Figure 9).[26] The concentrations of dyes in the desorbed solutions were determined spectrophotometrically. The best desorption was achieved with NaOH for both adsorbents. The desorption efficiency was up to 90% for ARS and 55% for XO in the case of MS-PEI adsorbent, while it was 40% for ARS and 20% for XO in the case of MS-APTES (Figure 9).

An effect of pH on the desorption of dyes in water was also investigated. The maximum desorption was observed at basic conditions, due to an increase in the negative species in the media as illustrated in Figure 10. In the case of MS-PEI at pH = 12, desorption was up to 90% for ARS and 54% for XO, whereas desorption percentage was up to 72% for ARS and 27% for XO in the case of MS-APTES.

dx.doi.org/10.1021/am500123k | ACS Appl. Mater. Interfaces 2014, 6, 4408−4417

Reusability. The primary advantage of adsorption over other processes is subjected to the recycling ability of the adsorbent. The reusability of adsorbent during the adsorption process reduces the operational cost. Therefore, the reusability of MS-PEI and MS-APTES for adsorption of dyes was studied. Desorption of the dyes from the loaded adsorbents was carried out by washing the particles with ethanol before each reusability cycle.[36] The results displayed in Figure 11 depict superior stability of MS-PEI during the adsorption−desorption cycle and show higher recycling capacity for ARS (7 cycles) and XO (5 cycles), as compared to MS-APTES, which was effective for up to 6 and 3 cycles for ARS and XO, respectively. Thus, MS-PEI is not merely efficient in adsorption but also possesses better potential for reusability.

CONCLUSIONS

A branched polymer PEI was covalently tethered at the surface of mesoporous silica to develop a novel adsorbent system, MS-PEI, for water remediation. The effectiveness of the employed strategy for the fabrication of mesoporous adsorbent material was supported by the ATR-FTIR, XPS, and TEM analyses. The adsorption studies of anionic dyes (ARS and XO) on MS-PEI and its monolayer analogue MS-APTES modified silica revealed the superior adsorption characteristics for MS-PEI, which can be attributed to the higher amine group density on the surface of adsorbent. The higher adsorption capacity toward both the dye molecules may be explained by the electrostatic nature of the interaction between the surface of the adsorbent and anionic dyes. The adsorption capacity was found to increase with the increase in adsorbent dosage and contact time. The solution pH has significant influence on the adsorption processes as an increase in the pH of the solutions led to a significant decrease in adsorption. Maximum adsorption against both adsorbents was achieved at room temperature that slightly decreased with an increase in temperature, reflecting on the exothermic adsorption behavior. The Freundlich model was found to be an appropriate model to explain the adsorption of dyes in both cases. The pseudo-second-order equation gave the better correlation for the adsorption data. The presented results highlight the relevance of the developed branched polymer functionalized mesoporous adsorbent material for environmental remediation by demonstrating the high removal efficiency, controlled adsorption−desorption characteristics, and most importantly reusability performances.

AUTHOR INFORMATION

Corresponding Author

*E-mail: yameen@mit.edu.

Present Address

[†]Laboratory of Nanomedicine and Biomaterials, MIT-Harvard Center for Cancer Nanotechnology Excellence, BWH, 75 Francis Street, Boston, MA 02115, USA.

Author Contributions

The manuscript was written through contributions of all authors. All authors have given approval to the final version of the manuscript.

Notes

The authors declare no competing financial interest.

ACKNOWLEDGMENTS

B.Y. acknowledges The Higher Education Commission (HEC) of Pakistan for Funding (Project No. 20-1799/R&D/10-5302) and LUMS for the Startup Grant. H.D. gratefully acknowledges The Scientific and Technological Research Council of Turkey (TUBITAK) for the financial support of Project No. 112M804.

REFERENCES

(1) Melero, J. A.; van Grieken, R.; Morales, G. Advances in the synthesis and catalytic applications of organosulfonic-functionalized mesostructured materials. *Chem. Rev.* **2006**, *106* (9), 3790−3812.

(2) Tang, F.; Li, L.; Chen, D. Mesoporous silica nanoparticles: Synthesis, biocompatibility and drug delivery. *Adv. Mater.* **2012**, *24* (12), 1504−1534.

(3) Sepehrian, H.; Fasihi, J.; Khayatzadeh Mahani, M. Adsorption behavior studies of picric acid on mesoporous MCM-41. *Ind. Eng. Chem. Res.* **2009**, *48* (14), 6772−6775.

(4) Ju, Y.; Webb, O.; Dai, S.; Lin, J.; Barnes, C. Synthesis and characterization of ordered mesoporous anion-exchange inorganic/organic hybrid resins for radionuclide separation. *Ind. Eng. Chem. Res.* **2000**, *39* (2), 550−553.

(5) Suteewong, T.; Sai, H.; Hovden, R.; Muller, D.; Bradbury, M. S.; Gruner, S. M.; Wiesner, U. Multicompartment mesoporous silica nanoparticles with branched shapes: An epitaxial growth mechanism. *Science* **2013**, *340* (6130), 337−341.

(6) Che, S.; Garcia-Bennett, A. E.; Yokoi, T.; Sakamoto, K.; Kunieda, H.; Terasaki, O.; Tatsumi, T. A novel anionic surfactant templating route for synthesizing mesoporous silica with unique structure. *Nat. Mater.* **2003**, *2* (12), 801−805.

(7) Tolbert, S. H.; Firouzi, A.; Stucky, G. D.; Chmelka, B. F. Magnetic field alignment of ordered silicate-surfactant composites and mesoporous silica. *Science* **1997**, *278* (5336), 264−268.

(8) He, H.-B.; Li, B.; Dong, J.-P.; Lei, Y.-Y.; Wang, T.-L.; Yu, Q.-W.; Feng, Y.-Q.; Sun, Y.-B. Mesostructured nanomagnetic polyhedral oligomeric silsesquioxanes (POSS) incorporated with dithiol organic anchors for multiple pollutants capturing in wastewater. *ACS Appl. Mater. Interfaces* **2013**, *5* (16), 8058−8066.

(9) Billinge, S. J.; McKimmy, E. J.; Shatnawi, M.; Kim, H.; Petkov, V.; Wermeille, D.; Pinnavaia, T. J. Mercury binding sites in thiol-functionalized mesostructured silica. *J. Am. Chem. Soc.* **2005**, *127* (23), 8492−8498.

(10) Aguado, J.; Arsuaga, J. M.; Arencibia, A.; Lindo, M.; Gascón, V. Aqueous heavy metals removal by adsorption on amine-functionalized mesoporous silica. *J. Hazard. Mater.* **2009**, *163* (1), 213−221.

(11) Anbia, M.; Salehi, S. Removal of acid dyes from aqueous media by adsorption onto amino-functionalized nanoporous silica SBA-3. *Dyes Pigm.* **2012**, *94* (1), 1−9.

(12) Walcarius, A.; Mercier, L. Mesoporous organosilica adsorbents: Nanoengineered materials for removal of organic and inorganic pollutants. *J. Mater. Chem.* **2010**, *20* (22), 4478−4511.

(13) Lam, K. F.; Yeung, K. L.; Mckay, G. Selective mesoporous adsorbents for and Cu 2+ separation. *Microporous Mesoporous Mater.* **2007**, *100* (1), 191−201.

(14) Huang, C.-H.; Chang, K.-P.; Ou, H.-D.; Chiang, Y.-C.; Chang, E.-E.; Wang, C.-F. Characterization and application of Ti-containing mesoporous silica for dye removal with synergistic effect of coupled adsorption and photocatalytic oxidation. *J. Hazard. Mater.* **2011**, *186* (2), 1174−1182.

(15) Li, S.; Jiao, X.; Yang, H. Hydrophobic core/hydrophilic shell structured mesoporous silica nanospheres: Enhanced adsorption of organic compounds from water. *Langmuir* **2013**, *29* (4), 1228−1237.

(16) Zhang, W.; Ye, G.; Chen, J. Novel mesoporous silicas bearing phosphine oxide ligands with different alkyl chains for the binding of uranium in strong HNO 3 media. *J. Mater. Chem. A* **2013**, *1* (41), 12706−12709.

(17) Lebed, P. J.; Savoie, J.-D.; Florek, J.; Bilodeau, F. o.; Larivière, D.; Kleitz, F. Large pore mesostructured organosilica-phosphonate hybrids as highly efficient and regenerable sorbents for uranium sequestration. *Chem. Mater.* **2012**, *24* (21), 4166−4176.

(18) Sanfeliu, C.; Martínez-Máñez, R.; Sancenón, F.; Soto, J.; Puchol, V.; Amorós, P.; Marcos, M. D. Low-cost materials for boron adsorption from water. *J. Mater. Chem.* **2012**, *22* (48), 25362−25372.
(19) Zou, Q.; Zou, L.; Tian, H. Detection and adsorption of Hg2+ by new mesoporous silica and membrane material grafted with a chemodosimeter. *J. Mater. Chem.* **2011**, *21* (38), 14441−14447.
(20) Zhuang, X.; Wan, Y.; Feng, C.; Shen, Y.; Zhao, D. Highly efficient adsorption of bulky dye molecules in wastewater on ordered mesoporous carbons. *Chem. Mater.* **2009**, *21* (4), 706−716.
(21) Donia, A. M.; Atia, A. A.; Al-amrani, W. A.; El-Nahas, A. M. Effect of structural properties of acid dyes on their adsorption behaviour from aqueous solutions by amine modified silica. *J. Hazard. Mater.* **2009**, *161* (2), 1544−1550.
(22) Wawrzkiewicz, M. Comparison of the efficiency of Amberlite IRA 478RF for acid, reactive, and direct dyes removal from aqueous media and wastewaters. *Ind. Eng. Chem. Res.* **2012**, *51* (23), 8069−8078.
(23) Chen, W.; Lu, W.; Yao, Y.; Xu, M. Highly efficient decomposition of organic dyes by aqueous-fiber phase transfer and in situ catalytic oxidation using fiber-supported cobalt phthalocyanine. *Environ. Sci. Technol.* **2007**, *41* (17), 6240−6245.
(24) Shi, B.; Li, G.; Wang, D.; Feng, C.; Tang, H. Removal of direct dyes by coagulation: The performance of preformed polymeric aluminum species. *J. Hazard. Mater.* **2007**, *143* (1), 567−574.
(25) Lee, J.-W.; Choi, S.-P.; Thiruvenkatachari, R.; Shim, W.-G.; Moon, H. Submerged microfiltration membrane coupled with alum coagulation/powdered activated carbon adsorption for complete decolorization of reactive dyes. *Water Res.* **2006**, *40* (3), 435−444.
(26) Afkhami, A.; Saber-Tehrani, M.; Bagheri, H. Modified maghemite nanoparticles as an efficient adsorbent for removing some cationic dyes from aqueous solution. *Desalination* **2010**, *263* (1), 240−248.
(27) Hoffmann, F.; Cornelius, M.; Morell, J.; Fröba, M. Silica-based mesoporous organic−inorganic hybrid materials. *Angew. Chem., Int. Ed.* **2006**, *45* (20), 3216−3251.
(28) Linares, N.; Serrano, E.; Rico, M.; Balu, A. M.; Losada, E.; Luque, R.; García-Martínez, J. Incorporation of chemical functionalities in the framework of mesoporous silica. *Chem. Commun.* **2011**, *47* (32), 9024−9035.
(29) Hu, L.-C.; Shea, K. J. Organo−silica hybrid functional nanomaterials: How do organic bridging groups and silsesquioxane moieties work hand-in-hand? *Chem. Soc. Rev.* **2011**, *40* (2), 688−695.
(30) Fujita, S.; Inagaki, S. Self-organization of organosilica solids with molecular-scale and mesoscale periodicities. *Chem. Mater.* **2008**, *20* (3), 891−908.
(31) Chaikittisilp, W.; Didas, S. A.; Kim, H.-J.; Jones, C. W. Vapor-phase transport as a novel route to hyperbranched polyamine-oxide hybrid materials. *Chem. Mater.* **2013**, *25* (4), 613−622.
(32) Yameen, B.; Ali, M.; Álvarez, M.; Neumann, R.; Ensinger, W.; Knoll, W.; Azzaroni, O. A facile route for the preparation of azide-terminated polymers."Clicking" polyelectrolyte brushes on planar surfaces and nanochannels. *Polym. Chem.* **2010**, *1* (2), 183−192.
(33) Lam, K. F.; Yeung, K. L.; Mckay, G. Efficient approach for Cd2+ and Ni2+ removal and recovery using mesoporous adsorbent with tunable selectivity. *Environ. Sci. Technol.* **2007**, *41* (9), 3329−3334.
(34) Lam, K. F.; Yeung, K. L.; McKay, G. An investigation of gold adsorption from a binary mixture with selective mesoporous silica adsorbents. *J. Phys. Chem. B* **2006**, *110* (5), 2187−2194.
(35) Bi, X.; Lau, R. J.; Yang, K.-L. Preparation of ion-imprinted silica gels functionalized with glycine, diglycine, and triglycine and their adsorption properties for copper ions. *Langmuir* **2007**, *23* (15), 8079−8086.
(36) Zhou, L.; Gao, C.; Xu, W. Magnetic dendritic materials for highly efficient adsorption of dyes and drugs. *ACS Appl. Mater. Interfaces* **2010**, *2* (5), 1483−1491.
(37) Maria Chong, A.; Zhao, X. Functionalization of SBA-15 with APTES and characterization of functionalized materials. *J. Phys. Chem. B* **2003**, *107* (46), 12650−12657.
(38) Roy, A.; Adhikari, B.; Majumder, S. B. Equilibrium, kinetic and thermodynamic studies of azo dye adsorption from aqueous solution by chemically modified lignocellulosic jute fiber. *Ind. Eng. Chem. Res.* **2013**, *52* (19), 6502−6512.
(39) Farrukh, A.; Akram, A.; Ghaffar, A.; Hanif, S.; Hamid, A.; Duran, H.; Yameen, B. Design of polymer-brush-grafted magnetic nanoparticles for highly efficient water remediation. *ACS Appl. Mater. Interfaces* **2013**, *5* (9), 3784−3793.
(40) Parida, K.; Mishra, K. G.; Dash, S. K. Adsorption of copper (II) on NH2-MCM-41 and its application for epoxidation of styrene. *Ind. Eng. Chem. Res.* **2012**, *51* (5), 2235−2246.
(41) Chatterjee, S.; Chatterjee, S.; Chatterjee, B. P.; Das, A. R.; Guha, A. K. Adsorption of a model anionic dye, eosin Y, from aqueous solution by chitosan hydrobeads. *J. Colloid Interface Sci.* **2005**, *288* (1), 30−35.
(42) Liu, J.; Ma, S.; Zang, L. Preparation and characterization of ammonium-functionalized silica nanoparticle as a new adsorbent to remove methyl orange from aqueous solution. *Appl. Surf. Sci.* **2013**, *265*, 393−398.
(43) Heydari-Gorji, A.; Belmabkhout, Y.; Sayari, A. Polyethylenimine-impregnated mesoporous silica: Effect of amine loading and surface alkyl chains on CO2 adsorption. *Langmuir* **2011**, *27* (20), 12411−12416.
(44) Gao, B.; Li, Y.; Chen, Z. Adsorption behaviour of functional grafting particles based on polyethyleneimine for chromate anions. *Chem. Eng. J.* **2009**, *150* (2), 337−343.
(45) Wang, X.; Ma, X.; Sun, L.; Song, C. A nanoporous polymeric sorbent for deep removal of H2S from gas mixtures for hydrogen purification. *Green Chem.* **2007**, *9* (6), 695−702.
(46) Gao, B.; An, F.; Liu, K. Studies on chelating adsorption properties of novel composite material polyethyleneimine/silica gel for heavy-metal ions. *Appl. Surf. Sci.* **2006**, *253* (4), 1946−1952.